Density Functional Theory Study of the Hydrogen-Bonded Pyridine−H_2O Complex: A Comparison with RHF and MP2 Methods and with Experimental Data

Ahmed Dkhissi,[†] **Ludwik Adamowicz,**[‡] **and Guido Maes***[,†]

Department of Chemistry, University of Leuven, Celestijnenlaan 200F, B3001, Heverlee, Belgium, and Department of Chemistry, University of Arizona, Tucson, Arizona 85721

Received: October 27, 1999

As a test for the applicability of the density functional theory (DFT) to hydrogen-bonded systems, various local and nonlocal exchange correlation functionals have been used to calculate the equilibrium structure and the harmonic vibrational frequencies of the pyridine−water complex. We also performed restricted Hartree−Fock (RHF) and Moller−Plesset (MP2) calculations for comparison. Three different basis sets (6-31G**, 6-31++G**, and 6-311++G(2d, 2p) 6d)) were used in the study. The best agreement between the DFT computed and the experimental rotational constants for monomeric pyridine were obtained with the B3-PW91 and B3-LYP functionals. For the vibrational frequencies of the H-bonded complex, the experimental data from matrix FT-IR spectrometry as well as the results obtained from the ab initio methods were best reproduced with the DFT method with the nonlocal exchange and correlation functionals. The hybrid approaches, which mix HF and Slater exchange, are particularly effective in these types of calculations.

Introduction

Investigations of hydrogen-bonded complexes using the density functional theory (DFT) have been performed extensively in recent years.[1−10] These include the theoretical DFT calculations of hydrogen-bonded systems involving the DNA bases. Some of these systems, as well as complexes of related model complexes, have been studied using both theoretical ab initio and experimental matrix-isolation FT-IR methodologies by the present authors.[11−19] Because of the extended amount of the theoretical results being available for these systems, the predictive ability of the theoretical methods including both ab initio and DFT techniques to describe structures and spectral properties of H-bonded systems can now be critically evaluated. In the present study, we have performed this evaluation for the pyridine−H_2O model system, which we have extensively studied in the past. Another motivating factor for the present study has been the recent demonstration that by modifying the DFT functional one can markedly improve the quality of the theoretical description of H-bonded complexes by the DFT method.[20,21] The experimental matrix FT-IR spectrum of the pyridine−H_2O complex was assigned based on the ab initio predicted energetic and spectral parameters of this system.[11] The relative simplicity of the pyridine−H_2O complex has allowed to perform both low- and high-level calculations including DFT and post Hartree−Fock (MP2) calculations. Last but not least, as we demonstrated, the properties of this complex are intermediate in a larger series of model H-bonded systems, including hydroxypyridines, pyrimidines, imidazoles, and benzimidazoles.[11−19] The conclusions of the present analysis can therefore be extrapolated to all the systems in the series.

Four main features have been used here to characterize the H-bond interaction in the pyridine−H_2O complex as well as in other H-bonding systems. These features are the length of the N···O intermolecular distance, the increase of the OH bond distance in the water molecule upon formation of the complex, the H-bond interaction energy, and the IR frequency shift of the stretching vibration of the OH proton donor group. The above quantities are either determined using theoretical ab initio or DFT calculations or taken from the experimental data. Among the different functionals used within the DFT method particulary the B3-LYP functional, which has been recommended by several authors,[4,7] has been thoroughly analyzed in combination with three different basis sets.

Details of Calculations

All calculations described in this paper were performed using the GAUSSIAN 94 program.[22] The DFT functionals used here were separated into exchange and correlation parts. The exchange functionals were those of Slater[23] and Becke.[24] The exchange Slater part, denoted by S, corresponds to the electron gas, while the Becke part, denoted by B, contains a gradient correction (nonlocal exchange). The correlation functionals are based on the local density approximation and on approximations based on the gradient corrections. The local density approximation is that proposed by Vosko, Wilk, and Nusair (VWN)[25] and corresponds to the parametrization of the correlation energy of the homogeneous electron gas. For the gradient-corrected approximation, we have considered both the gradient-corrected functional of Lee, Yang, and Parr (LYP)[26a] and the Perdew and Wang gradient-corrected correlation functional (PW91).[26b]

The exchange functionals can be combined with different local or gradient-corrected correlation functionals. The notation originally proposed by Pople and co-workers[27] has been adopted here. In this notation, the X−C symbol is used, where X denotes the exchange functional type and C denotes the correlation functional type. For example, B-LYP denotes the Becke exchange functional combined with the Lee−Yang−Parr correlation functional.

Hybrid methods, which include a mixture of the HF exchange functional with the DFT exchange correlation functional, are

---

[†] University of Leuven.
[‡] University of Arizona.

10.1021/jp9938056 CCC: $19.00

also analyzed in this study. The two hybrid methods suggested by Becke[28,29] are used. In the first method equal contributions from both Hartree−Fock exchange and Slater exchange[28] functionals are combined with the LYP correlation functional to form the BH&H functional (BHH-LYP). The second functional is the Becke3 functional where the exchange part consists of contributions from the Slater and Hartree−Fock exchange functionals and from Becke's 1988 gradient correction functional.[30] This functional is combined with the LYP and PW91 correlations functionals. In this work, we also consider a modified functional which is obtained from the B3-LYP and B3-PW91 functionals according to the following expression:

$$E_{\mathrm{XC}} = E_{\mathrm{XC}}^{\mathrm{LSDA}} + a_0(E_{\mathrm{X}}^{\mathrm{exact}} - E_{\mathrm{X}}^{\mathrm{LSDA}}) + a_{\mathrm{X}}\Delta E_{\mathrm{X}}^{\mathrm{B88}} + a_{\mathrm{c}}\Delta E_{\mathrm{C}}^{\mathrm{NL}}$$

In this modification, the original Becke3 parameters (a_0, a_x, a_c = 0.20, 0.72, 0.81) are replaced by $a_0 = 0.35$, $a_x = 0.72$, and $a_c = 0.81$, as suggested by Latajka and co-workers.[20] This modified functional is denoted as Becke3(M).

To compare the DFT and ab initio results, HF and MP2 calculations were performed. In the calculations, the 6-31++G** basis set was employed for the molecular orbital expansion. Two other basis sets were also used in the B3-LYP calculations to determine the basis set dependency of the DFT results. By using a smaller 6-31G** basis set and comparing the results with the results obtained with the 6-31++G** basis we were able to estimate the importance of the diffuse functions. By using a larger 6-311++G(2d,2p) basis set with several additional polarization functions, which were used before in studies of the H_2O−CO,[9] $(HF)_2$,[3] and $(FHF)^-$ [20] complexes, we determined the importance of using more than one polarization function in the DFT calculations.

In calculating the interaction energy of the complex, we accounted for the basis set superposition error (BSSE) by recalculating the monomer energies in the basis set of the heterodimer using the so-called counterpoise method.[31,32] With these energies, the BSSE corrected interaction energy is then calculated as

$$\Delta E_{\mathrm{A\cdots B}} = E_{\mathrm{A\cdots B}} - E_{\mathrm{A(B)}} - E_{\mathrm{B(A)}}$$

where E $_{\mathrm{A\cdots B}}$ is the energy of the dimer, E_{A} is the energy of the monomer A obtained with the extra ghost Gaussian functions placed at the positions of the nuclei of B in the dimer, and E_{B} is the energy of the monomer B obtained with the extra ghost Gaussian functions placed at the positions of the nuclei of A in the dimer. The interaction energy was corrected for the zero-point vibrational energy (ZPE) calculated using the harmonic approximation and scaled with single scaling factors equal to 0.90 for HF, 0.95 for DFT, and 0.96 for MP2. The IR frequencies and intensities were computed analytically for HF and DFT and numerically for MP2.

Results and Discussions

A. Monomer H_2O. In Table 1, we present the structural and vibrational parameters for the monomer H_2O molecule obtained with the DFT method. For the sake of comparison, the results of the HF and MP2 calculations and the experimental results are also given.

The results in Table 1 indicate that the OH bond length predicted by the different DFT methods is too long by 0.01−0.02 Å in comparison with the experimental data or with those calculated at the MP2 level of theory. On the other hand, DFT with the B3(M)-PW91 and BH&H functionals underestimates the OH bond length by 0.0013 and 0.0039 Å, respectively. It can be noticed that enlarging of the basis set to 6-311++G(2d, 2p) improves the agreement with the experiment. The H−O−H angle, calculated using different functionals, is in good agreement with both the experiment and the MP2 results.

TABLE 1: Structural and Vibrational Properties for the H_2O Molecule Calculated with the 6-31++G Basis Set**

	r (Å)	α (deg)	μ (D)	ν_1 (cm^{-1})	ν_2 (cm^{-1})	ν_3 (cm^{-1})
S-VWN	0.9727	105.9	2.24	3735	1524	3867
S-LYP	0.9783	106.0	2.25	3684	1495	3817
B-VWN	0.9705	105.0	2.14	3702	1595	3824
B-LYP	0.9759	105.0	2.16	3655	1567	3777
B3-LYP	0.9653	105.7	2.19	3805	1601	3927
B3-LYP[e]	0.9653	103.7	2.04	3800	1666	3912
B3-LYP[f]	0.9609	105.1	1.96	3820	1639	3921
B3(M)-LYP	0.9584	106.0	2.19	3897	1638	4017
B3−PW91	0.9627	105.6	2.19	3845	1606	3971
B3(M)-PW91	0.9559	105.8	2.19	3936	1644	4059
BH&H	0.9533	106.5	2.21	3980	1652	4102
HF	0.9433	107.1	2.23	4146	1728	4269
MP2	0.9633	105.4	2.28	3865	1619	4012
exptl	0.9572[a]	104.5[a]	1.855[b]	3832[c]	1649[c]	3942[c]
				3657[d]	1595[d]	3756[d]

[a] Reference 41. [b] Reference 42. [c] Reference 43 (harmonic frequencies). [d] Reference 44 (anharmonic frequencies). [e] Calculated with the 6-31G** basis set. [f] Calculated with the 6-311++G(2d,2p) basis set.

TABLE 2: Rotational Constants and Dipole Moment for the Pyridine Molecule Calculated with the 6-31++G Basis Set**

	A (MHz)	B (MHz)	C (MHz)	mean deviation	μ (D)
S-VWN	6059.732	5839.787	2973.864	23	2.39
S-LYP	6038.954	5825.290	2965.099	10	2.39
B-VWN	5947.971	5714.901	2914.554	75	2.34
B-LYP	5930.634	5700.714	2906.701	31	2.35
B3-LYP	6022.167	5798.198	2954.030	10	2.37
B3-LYP[a]	6037.970	5806.191	2959.906	1	2.18
B3-LYP[b]	6076.444	5855.636	2981.999	37	2.30
B3(M)-LYP	6060.966	5839.870	2974.182	24	2.38
B3-PW91	6045.387	5816.394	2964.340	72	2.36
B3(M)-PW91	6084.192	5855.467	2983.819	40	2.37
BH&H	6115.2698	5900.6900	3003.0320	72	2.39
HF	6132.755	5917.601	3011.629	86	2.40
MP2	6015.468	5777.688	2947.091	18	2.46
exptl	6039.244	5804.903	2959.220		2.15
	(0.011)[c]	(0.011)[c]	(0.008)[c]		(0.05)[d]

[a] Calculated with the 6-31G** basis set. [b] Calculated with the 6-311++G(2d, 2p) basis set. [c] Reference 45. [d] Reference 46.

The dipole moment is not very sensitive to the choice of the functional in the DFT method, but it is sensitive to the choice of the basis set. The value calculated with the 6-311++G(2d, 2p) basis set is close to the experimental value.

For the vibrational modes ν_1, ν_2, and ν_3, the observed fundamental (anharmonic) and the calculated harmonic frequencies are also listed in Table 1. As known, the HF method overestimates vibrational frequencies, whereas the MP2 calculations are usually in a better agreement with the experimental frequencies. The DFT values are too low compared to the experimental frequencies, though the results computed with the B3-LYP and B3-PW91 functionals are in good agreement with the MP2 and experimental vibrational values. Also, in this case the results improve when the larger basis set is used.

B. Monomer Pyridine. *Structural Properties.* The ground state rotational constants and the dipole moment for pyridine calculated with DFT methods are reported in Table 2. The experimentally determined rotational constants, as well as the results of the HF and MP2 calculations, are also presented in the table for comparison. The first observation one makes is

TABLE 3: Experimental (Ar Matrix) and Calculated Vibrational Properties of Pyridine

ν (cm^{-1}) exptl	ν (cm^{-1}) B3-PW91[a]	ν (cm^{-1}) B3-LYP[b]	ν (cm^{-1}) B3(M)-LYP[c]	ν (cm^{-1}) MP2[d]	PED[e]	PED B3-PW91	PED B3-LYP	PED B3(M)-LYP	PED MP2
3059	3224	3210	3271	3282	$\nu(C_3H)$	33	34	33	31
	3047	3050	3042	3052	$\nu(C_4H)$	30	31	28	31
					$\nu(C_5H)$	33	31	33	31
3039	3216	3202	3264	3274	$\nu(C_5H)$	48	48	47	46
	3039	3042	3036	3045	$\nu(C_3H)$	48	46	47	46
3028	3200	3187	3248	3260	$\nu(C_4H)$	68	66	67	60
	3024	3028	3021	3032					
2996	3179	3169	3233	3248	$\nu(C_6H)$	45	52	40	40
	3004	3011	3007	3021	$\nu(C_2H)$	46	34	41	31
3008	3177	3168	3231	3247	$\nu(C_2H)$	48	57	46	50
	3002	3010	3005	3020	$\nu(C_6H)$	48	38	47	41
1582	1646	1632	1671	1650	$\nu(C_2C_3)$	23	23	22	23
	1605	1591	1587	1601	$\nu(C_5C_6)$	23	23	22	23
1577	1641	1627	1664	1642	$\nu(C_3C_4)$	24	24	23	26
	1600	1586	1581	1593	$\nu(C_4C_5)$	13	23	23	26
1483	1518	1516	1553	1527	$\delta(C_2H)$	20	21	20	24
	1480	1478	1475	1481	$\delta(C_6H)$	20	21	20	24
1441	1478	1475	1509	1493	$\delta(C_4H)$	19	20	20	18
	1441	1438	1434	1448	$\nu(C_2C_3)$	14	13	13	18
					$\nu(C_5C_6)$	14	13	13	18
1363	1381	1386	1420	1398	$\delta(C_2H)$	33	33	33	25
	1346	1351	1349	1356	$\delta(C_6H)$	33	33	33	25
1226	1329	1304	1304	1411	$\nu(N_1C_2)$	27	27	26	20
	1296	1271	1239	1369	$\nu(C_6N_1)$	27	27	26	20
1218	1247	1244	1271	1259	$\delta(C_2H)$	23	21	21	20
	1216	1213	1207	1221	$\delta(C_6H)$	23	21	21	20
1146	1172	1172	1193	1193	$\delta(C_4H)$	40	38	34	41
	1143	1143	1133	1157	$\delta(C_5H)$	20	20	18	21
					$\delta(C_3H)$	20	20	18	21
1073	1097	1094	1116	1104	$\delta(C_5H)$	20	18	18	16
	1070	1067	1060	1071	$\delta(C_3H)$	20	18	18	16
					$\nu(C_4C_5)$	13	13	13	16
					$\nu(C_3C_4)$	13	13	13	16
1051	1084	1079	1101	1092	$\nu(C_2C_3)$	23	24	24	23
	1057	1052	1046	1059	$\nu(C_5C_6)$	23	24	24	23
1031	1049	1046	1065	1052	δ_{R1}	30	42	46	50
	1023	1020	1012	1020	$\nu(C_4C_5)$	18	17	16	14
[f]	1010	1011	1041	892	$\gamma(C_4H)$	56	56	57	37
	988	991	999	892	$\gamma(C_3H)$	28	28	28	
					$\gamma(C_5H)$	28	28	28	36
					$\gamma(C_2H)$				
991	1013	1011	1031	1013	δ_{R1}	59	43	39	36
	983	986	979	983	$\nu(N_1C_2)$	12	14	14	17
947	1000	999	1030	889	$\gamma(C_2H)$	43	43	43	54
	980	979	989	889	$\gamma(C_6H)$	43	42	43	54
[g]	958	958	986	867	$\gamma(C_2H)$	39	39	40	
	939	939	947	867	$\gamma(C_6H)$	39	39	40	
					$\gamma(C_3H)$	27	27	26	32
					$\gamma(C_4H)$				32
					$\gamma(C_5H)$				23
[g]	894	894	917	835	$\gamma(C_5H)$	40	40	40	55
	876	876	880	835	$\gamma(C_5H)$	40	40	40	55
745	758	757	776	517	τ_{R1}	79	73	66	51
					τ_{R3}				26
702	713	714	730	710	τ_{R1}	43	48	55	
	699	700	701	710	$\gamma(C_3H)$	16	15	13	20
					$\gamma(C_5H)$	16	15	13	20
					$\gamma(C_4H)$	12	11	10	33
659	665	668	681	664	δ_{R3}	91	91	91	91
	648	651	647	644					
602	609	613	626	608	δ_{R2}	93	92	92	92
	594	598	595	590					
g	414	417	429	280	τ_{R3}	82	82	82	58
	406	409	412	280	τ_{R2}	27	27	27	19
					τ_{R1}				35
407	378	382	397	338	τ_{R2}	85	85	85	88
	370	374	381		τ_{R3}	28	28	28	29

[a] First row, unscaled value; second row, scaling factor 0.945 for ν(XH), 0.980 for γ and τ, and 0.975 for other vibrational modes. [b] First row, unscaled value; second row, scaling factor 0.950 for ν(XH), 0.980 for γ and τ, and 0.975 for other vibrational modes. [c] First row, unscaled value; second row, scaling factor 0.930 for ν(XH), 0.960 for γ and τ, and 0.950 for other vibrational modes. [d] First row, unscaled value; second row, scaling factor 0.930 for ν(XH), 1.000 for γ and τ, and 0.970 for other vibrational modes. [e] Only PED contributions ≥ 15 are listed in the last four colums. [f] Intensity too low to be observed. [g] IR inactive a_2 mode.

TABLE 4: Selected Intermolecular and Intramolecular Structural Data for the Equilibrium Complex Pyridine−H_2O[a]

	R(N−O)	$r(OH_b)$	$\Delta r(OH_b)$	$r(OH_f)$	$-\Delta r(OH_f)$	$C_2N_1H_{12}$	$N_1H_{12}O_{13}$
S-VWN	2.66	1.0047	0.0320	0.9713	0.0014	140	155
S-LYP	2.60	1.0137	0.0354	0.9762	0.0021	143	148
B-VWN	3.01	0.9840	0.0135	0.9697	0.0008	122	179
B-LYP	2.92	0.9934	0.0175	0.9749	0.0010	121	177
B3-LYP	2.91	0.9807	0.0154	0.9644	0.0009	122	179
B3-LYP[b]	2.88	0.9765	0.0112	0.9651	0.0002	143	152
B3-LYP[c]	2.91	0.9764	0.0155	0.9599	0.0010	121	177
B3(M)-LYP	2.96	0.9704	0.0120	0.9573	0.0011	122	179
B3-PW91	2.90	0.9794	0.0167	0.9619	0.0008	122	179
B3(M)-PW91	2.95	0.9689	0.0130	0.9550	0.0009	121	179
BH&H	2.91	0.9661	0.0128	0.9524	0.0009	122	179
HF	3.06	0.9507	0.0074	0.9425	0.0008	120	178
MP2	2.92	0.9771	0.0138	0.9629	0.0004	121	177

[a] Distances in angstroms; angles in degrees. OH_b is the bond involved in the H-bond while OH_f is the free bond. [b] Calculated with the 6-31G** basis set. [c] Calculated with the 6-311++G(2d, 2p) basis set.

that the MP2 results reproduce the experimental constants more accurately than the HF results.

To compare all the methods, we calculated the mean deviation between the experimental and the calculated values. The mean deviations for the predicted rotational constants are 23, 10, 75, 31, 10, 24, 7, 40, 72, 86, and 18 MHz for DFT with the S-VWN, S-LYP, B-VWN, B-LYP, B3-LYP, B3(M)-LYP, B3-PW91, B3-(M)-PW91, and BH&H functionals and for the HF and MP2, respectively. These values indicate that the agreement between the calculated and the experimental rotational constants decreases in the following order: DFT(B3-PW91) (the best agreement) → DFT(B3-LYP) → DFT(S-LYP) → MP2 → DFT-(S-VWN) → DFT(B3(M)-LYP) → DFT(B-LYP) → DFT(B3-(M)-PW91) → DFT(BH&H) → DFT(BVWN) → HF (the worth agreement). DFT with the B3-PW91 functional gives slightly better results than DFT(B3-LYP) and MP2. The comparison indicates that DFT(B3-PW91) and DFT(B3-LYP) are probably the best functionals to calculate equilibrium structures of the heterocyclic bases including the nucleic acid bases. The DFT-(B3-PW91) and DFT(B3-LYP) optimized geometries are very close to the experimental results and to the MP2 calculated values.

The DFT(B3-LYP) rotational constants calculated with various basis sets are similar, although the DFT(B3-LYP)/6-31G** results are slightly better than the others. The 6-31G** basis set seems to be sufficient to predict structures and related properties of larger monomeric molecules, but as we demonstrate next, to obtain reliable vibrational information for H-bonded systems, additional diffuse functions in the basis set are necessary.

Vibrational Properties. The vibrational analysis of the pyridine experimental spectrum is summarized in Table 3 and compared with predicted frequency values obtained with different calculation methods (B3-PW91, B3-LYP, MP2 and B3-(M)-LYP).

In our earlier report,[11] all the modes calculated at the HF level of theory were scaled down by the single scaling factor of 0.90 to approximately correct for the anharmonicity of the vibrations and for overstimation of the force constants by the HF method. The mean deviation between the experimental frequencies (accuracy 1 cm^{-1}) and ab initio frequencies after scaling was 18.1 cm^{-1}. A single scaling factor for correlated methods does not take into account that the anharmonicity contributions are not uniform over the whole range of the vibrational modes. The use of different scaling factors for frequencies belonging to different types of vibrational modes has been proposed by several authors.[19,33−34] Following this approach, the following different scaling factors were used in this work for the different theoretical methods and for different vibrational modes: for DFT(B3-LYP), 0.975 for all modes except ν_{XH} and γ_R, τ_R modes where the scaling factors of 0.950 and 0.980 were applied; for DFT(B3-PW91), 0.945 for ν_{XH}, 0.980 for $\gamma_{R,}$, τ_R, and 0.975 for all other modes; for DFT(B3-(M)-LYP), 0.930 for ν_{XH}, 0.960 for $\gamma_{R,}$, τ_R, and 0.950 for all other modes; for MP2, 0.930 for ν_{XH}, 1.00 for $\gamma_{R,}$, τ_R, and 0.970 for all other modes.

It can be seen that the scaling factors used for the DFT(B3-PW91) method are very close to those in the DFT(B3-LYP) method while for ν_{XH} modes the scaling factor used for the DFT-(B3(M)-LYP) method is equal to that of the MP2 method. When different scaling factors are used, the mean frequency deviation is 10 cm^{-1} for DFT(B3-LYP), 11.5 cm^{-1} for DFT(B3(M)-LYP), 13.4 cm^{-1} for DFT(B3−PW91), and 29 cm^{-1} for the MP2 level of theory when the 6-31++G** basis set is used in the calculations. The mean frequency deviation obtained here with the B3-LYP functional in the DFT method and with the MP2 method are very close to the results obtained for imidazole.[17]

It appears that the MP2/6-31++G** level of theory yields incorrect results for the two modes experimentally observed at 1226 and 745 cm^{-1}. The calculated frequencies are about 143 cm^{-1} too high and 228 cm^{-1} too low, respectively. A similar effect has also been reported for similar modes commonly denoted as ν_4 and ν_{14} in benzene[35,36] and in phenol.[37] Handy et al.[35] have shown that the error in the mode ν_4 can be corrected by including f basis functions in the MP2 calculation. On the other hand, the DFT predictions for these modes are in good agreement with the experimental results. If these modes are excluded from the analysis, the mean deviation of the MP2 frequencies reduces to about 14 cm^{-1}.

The mean frequency deviation obtained with the DFT and the B3-LYP functional are 10, 10, and 8 cm^{-1} with the 6-31G**, 6-31++G**, and 6-311++G(2d,2p) basis sets, respectively. Clearly, the use of a larger basis set leads to slightly better results in this case.

C. Complex Pyridine−H_2O. *Structural Properties.* Table 4 presents the computed selected intermolecular and intramolecular structural data for the pyridine−H_2O complex.

The MP2 calculated H-bond distance (N···O) is 2.92 Å. This distance is shorter than that obtained at the RHF level (3.06 Å), indicating the importance of the correlation effects. The N···O intermolecular distance calculated with the S-VWN and S-LYP functionals in DFT is largely underestimated by about 0.3 Å in comparison to the MP2 result, while DFT with the B-VWN functional overestimates this value by 0.09 Å. This situation is similar as for the simple hydrogen-bonded complexes $(H_2O)_2$[7] and $(HF)_2$.[3] DFT with the nonlocal B-LYP functional

TABLE 5: Total Energy (au) and Interaction Energy (kJ/mol) for the Pyridine−H_2O Complex

	H_2O	pyridine	pyridine−H_2O	ΔE	ΔE + BSSE	ΔE_c[a]
S-VWN	−76.0662283	−246.8919556	−322.9788175	−54.17	−52.71	−46.27
S-LYP	−75.5502056	−244.7812704	−320.3573355	−67.89	−66.32	−58.74
B-VWN	−76.933447	−250.3181946	−327.2596524	−21.03	−19.54	−12.80
B-LYP	−76.4162291	−248.2014366	−324.5502635	−28.04	−26.56	−19.58
B3-LYP	−76.4341236	−248.3034434	−324.7486828	−29.18	−27.75	−20.58
B3-LYP[b]	−76.4197365	−248.2926016	−324.725458	−34.45	−22.00	−13.31
B3-LYP[c]	−76.4627964	−248.3641133	−324.837053	−26.63	−26.02	−18.79
B3(M)-LYP	−76.5570327	−248.8034468	−325.3703370	−25.88	−24.30	−16.94
B3-PW91	−76.4046866	−248.2038626	−324.618903	−27.18	−25.61	−18.50
B3(M)-PW91	−76.5280260	−248.7046034	−325.2417136	−23.85	−22.14	−15.08
BH&H	−76.3910509	−248.1478334	−324.5502635	−29.88	−28.23	−19.51
HF	−76.0313091	−246.7123953	−322.7523520	−22.73	−21.05	−14.48
MP2	−76.2333759	−247.5374741	−323.7834202	−33.00	−26.32	−18.92

[a] $\Delta E_c = \Delta E + \text{BSSE} + \Delta\text{ZPE}$, with ZPE calculated as $0.95\sum h\nu_i/2$, $0.90\sum h\nu_i/2$, $0.96\sum h\nu_i/2$ for DFT, HF, and MP2, respectively (ν_i are the frequencies). [b] Calculated with the 6-31G** basis set. [c] Calculated with the 6-31++G(2d, 2p) basis set.

SCHEME 1: Structure of the Pyridine−H_2O Complex

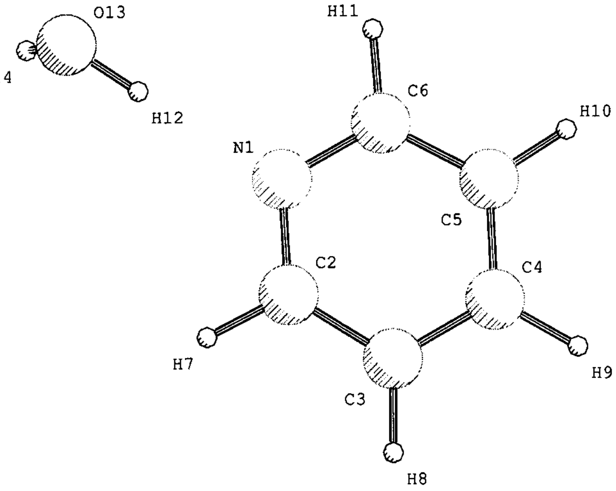

TABLE 6: Harmonic Vibrational Frequencies (ν_c, cm^{-1}) and Frequency Differences ($\Delta\nu = \nu_c - \nu_m$)[a] for the Fundamental Vibrations of H_2O in the Complex with Pyridine Calculated with the 6-31++G Basis Set**

	ν_1	$\Delta\nu_1$	ν_2	$\Delta\nu_2$	ν_3	$\Delta\nu_3$
S-VWN	3181	−554	1569	+45	3820	−47
S-LYP	3090	−594	1556	+61	3778	−39
B-VWN	3480	−222	1628	+33	3779	−45
B-LYP	3359	−296	1598	+31	3732	−45
B3-LYP	3538	−267	1638	+37	3881	−46
B3-LYP[c]	3631	−169	1694	+28	3865	−47
B3-LYP[d]	3542	−278	1669	+30	3884	−37
B3(M)-LYP	3693	−204	1675	+37	3976	−41
B3-PW91	3554	−291	1644	+38	3921	−50
B3(M)-PW91	3715	−221	1681	+37	4015	−44
BH&H	3758	−222	1691	+39	4058	−44
HF	4038	−108	1766	+38	4232	−37
MP2	3635	−230	1664	+45	3954	−58
exptl[b]	3400	−271	1616	+26	3701	−36

[a] ν_c denotes the complex frequency, and ν_m the monomer frequency. [b] Experimental anharmonic frequencies from ref 11. [c] Calculated with the 6-31G** basis set. [d] Calculated with the 6-311++G(2d, 2p) basis set.

and with all the hybrid functionals predicts the N···O intermolecular distance in good agreement with the MP2 value.

Using a larger basis set in DFT calculations with different functionals does not noticeably alter the N···O intermolecular distance in comparison to the results obtained with the 6-31++G** basis. However, using the 6-31G** basis without diffuse functions leads to a shorter N···O intermolecular distance.

The second interesting structural feature is the elongation of the OH bond upon formation of the H-bonded complex. As a matter of fact, this parameter is the key factor affecting the predicted infrared properties of hydrogen-bonded complexes. The OH bond elongation is sensitive to the type of functional used in the DFT method and it is usually larger than calculated at the MP2 level. The values calculated with DFT(BH&H), DFT(B-VWN), and DFT (B3(M)) are the closest to the results obtained in the MP2 calculations.

The $N_1H_{12}O_{13}$ angle (Scheme 1) computed with most of the DFT functionals considered here, except for the S-VWN and S-LYP functionals, is in good agreement with the MP2 result. The situation is similar for the $C_2N_1H_{12}$ angle.

Interaction Energy. The interaction energy, ΔE, for the complex ($\Delta E = E^{\text{complex}} - E^{\text{H}_2\text{O}} - E^{\text{pyridine}}$) calculated using 13 different methods is presented in Table 5. Corrections for the basis set superposition error (BSSE) and for the zero-point vibrational energy are also given.

It can be seen that the interaction energy calculated with the DFT(S-VWN) method is much larger than that obtained with the MP2 method. On the other hand, DFT with the B-VWN functional understimates this energy. These results agree with the results obtained for simple hydrogen-bonded systems by Sim et al.,[1] Latajka et al.,[3] Hobza et al.,[38] and Novoa et al.[7]

The interaction energy obtained with the nonlocal B-LYP functional is −28.04 kJ/mol compared to −33 kJ/mol obtained at the MP2 level. The agreement between DFT(B-LYP) and MP2 is much better when the basis set superposition error (BSSE) correction is taken into account. This correction is 1.48 kJ/mol for the DFT method with the B-LYP functional, which is similar to the corrections obtained at the HF level and those obtained with DFT with other functionals but substantially smaller than the value 6.7 kJ/mol obtained at the MP2 level. This amount of correction is consistent with the results obtained by Xantheas et al.[8] The BSSE correction of the DFT functionals for the 6-31++G** basis set is practically constant and oscillates between 1.43 for DFT(B3-LYP) and 1.71 kJ/mol for DFT(B3(M)-LYP). These results confirm the results obtained by Novoa et al.[7] The BSSE corrected values for the interaction energy are −26.56 and −26.32 kJ/mol at the DFT(B-LYP) and MP2 levels, respectively. Using standard hybrid functionals, the BSSE corrected interaction energy ranges from −25.61 kJ/mol (DFT(B3-PW91)) to −28.23 kJ/mol (DFT(BH&H)). These values are in good agreement with the MP2 result. On the other hand, the BSSE corrected energy interaction energy obtained with DFT and the modified hybrid functional is below the value of MP2.

TABLE 7: Experimental (Ar Matrix) and Vibrational Properties of Pyridine−H_2O

ν (cm^{-1}) exptl	ν (cm^{-1}) B3-PW91[a]	ν (cm^{-1}) B3-LYP[b]	ν (cm^{-1}) B3(M)-LYP[c]	ν (cm^{-1}) MP2[d]	PED[e]	PED B3-PW91	PED B3-LYP	PED B3(M)-LYP	PED MP2
3701	3922	3881	3976	3954	ν^f(OH)	82	81	76	74
	3706	3687	3698	3677	ν^b(OH)	19	19	24	26
3400	3554	3538	3693	3635	ν^b(OH)	81	81	24	74
	3359	3361	3435	3381	ν^f(OH)	19	19	76	26
1616	1644	1638	1675	1664	δ (HOH)	59	80	87	87
	1603	1597	1591						
575	748	739	710	736	δ(OH···N)	97	97	90	97
	729	720		714					
f	370	364	354	365	γ(OH···N)	38	48	64	85
	363	357	340	365	oop butterfly	28	24	16	
f	147	148	139	151	ν(OH···N)	96	96	97	96
	143	144	132	146					
f	105	109	106	106	τ(OH···N)	97	98	98	98
	103	107	102	106					
f	44	43	42	36	oop butterfly	103	104	104	103
	43	42	40	36					
f	27	26	26	8	ip butterfly	98	98	98	99
	26	25	25	8					
3060(+1)	3227(+3)	3215(+5)	3275(+4)	3286(+4)	$\nu(C_3H)$	35	34	34	33
	3050	3054	3046	3056	$\nu(C_4H)$	25	25	24	28
					$\nu(C_5H)$	35	35	35	33
3041(+2)	3221(+5)	3209(+7)	3269(+5)	3279(+5)	$\nu(C_5H)$	47	46	45	45
	3044	3049	3040	3049	$\nu(C_3H)$	47	47	46	45
3031(+3)	3204(+4)	3193(+6)	3252(+4)	3264(+4)	$\nu(C_4H)$	69	67	65	60
3012(+4)	3191(+12)	3181(+12)	3242(+9)	3254(+6)	$\nu(C_6H)$	62	61	72	51
	3015	3022	3015	3026	$\nu(C_2H)$	19	16		40
g	3190(+13)	3180(+12)	3241(+10)	3253(+6)	$\nu(C_2H)$	69	69	79	38
	3015	3021	3014	3025	$\nu(C_6H)$	25	23		27
1589(+7)	1653(+7)	1640(+8)	1677(+6)	1658(+8)	$\nu(C_2C_3)$	23	21	22	23
	1612	1599	1593	1608	$\nu(C_5C_6)$	23	21	22	23
1577(+0)	1643(+2)	1628(+1)	1665(+1)	1643(+1)	$\nu(C_3C_4)$	15	24	23	26
	1602	1587	1582	1594	$\nu(C_4C_5)$	17	23	23	26
1484(+1)	1521(+3)	1519(+3)	1556(+3)	1530(+3)	$\delta(C_2H)$	19	20	20	23
	1483	1481	1478	1483	$\delta(C_6H)$	19	20	20	23
1443(+2)	1481(+3)	1479(+4)	1512(+3)	1497(+4)	$\delta(C_4H)$	19	20	20	17
	1444	1442	1436	1452	$\nu(C_2C_3)$	15	14	13	19
					$\nu(C_5C_6)$	15	14	13	19
g	1382(+1)	1387(+1)	1421(+1)	1399(+1)	$\delta(C_2H)$	32	33	33	28
	1347	1352	1350	1357	$\delta(C_6H)$	32	33	33	28
1227(+1)	1335(+6)	1309(+5)	1308(+4)	1417(+6)	$\nu(N_1C_2)$	27	28	26	23
	1302	1276	1243	1374	$\nu(C_6N_1)$	27	27	26	23
g	1246(−1)	1244(+0)	1272(+1)	1258(−1)	$\delta(C_2H)$	23	22	21	20
	1215	1213	1208	1220	$\delta(C_6H)$	23	22	21	20
1146(+0)	1175(+3)	1175(+3)	1196(+3)	1196(+3)	$\delta(C_4H)$	39	38	34	40
	1146	1146	1136	1220	$\delta(C_5H)$	20	20	18	21
					$\delta(C_3H)$	20	20	18	21
1071(−2)	1098(+1)	1094(+0)	1117(+1)	1104(+0)	$\delta(C_5H)$	19	18	17	16
	1071	1067	1061	1071	$\delta(C_3H)$	20	18	18	16
1053(+2)	1090(+6)	1085(+6)	1106(+5)	1098(+6)	$\nu(C_2C_3)$	23	23	24	23
	1063	1058	1051	1065	$\nu(C_5C_6)$	23	23	24	23
1033(+2)	1049(+0)	1046(+0)	1066(+1)	1051(−1)	δ_{R1}	32	51	56	59
	1023	1020	1013	1019	$\nu(C_4C_5)$	18	15	13	12
					$\nu(C_3C_4)$	18	15	13	12
g	1012(+2)	1013(+2)	1042(+1)	897(+5)	$\gamma(C_4H)$	60	60	60	48
	992	992	1000	897	$\gamma(C_3H)$	27	27	27	
					$\gamma(C_5H)$	28	27	27	
					$\gamma(C_6H)$				38
					$\gamma(C_2H)$				24
1000(+9)	1023(+10)	1021(+10)	1040(+9)	1024(+11)	δ_{R1}	58	36	31	29
	997	995	988	993	$\nu(N_1C_2)$	10	14	14	16
g	1000(+0)	999(+0)	1030(+0)	895(+6)	$\gamma(C_2H)$	41	41	41	61
	980	979	989	895	$\gamma(C_6H)$	42	42	42	47
g	961(+3)	961(+3)	989(+3)	872(+5)	$\gamma(C_2H)$	41	41	41	10
	942	942	949	872	$\gamma(C_6H)$	40	40	40	
					$\gamma(C_4H)$	23	23	23	22
					$\gamma(C_5H)$				24
					$\gamma(C_3H)$				24
g	895(+1)	895(+1)	918(+1)	847(+12)	$\gamma(C_3H)$	39	39	39	54
	877	877	881	847	$\gamma(C_5H)$	39	39	39	54
749(+4)	759(+1)	758(+1)	778(+2)	518(+1)	τ_{R1}	65	60	55	51
	744	743	747	518					
699(−3)	712(−1)	712(−3)	728(−2)	715(+5)	τ_{R1}	56	60	65	
	698	695	699	715	$\gamma(C_3H)$	13	12	10	20
					$\gamma(C_5H)$	13	12	11	20

TABLE 7: (Continued)

ν (cm^{-1}) exptl	ν (cm^{-1}) B3-PW91[a]	ν (cm^{-1}) B3-LYP[b]	ν (cm^{-1}) B3(M)-LYP[c]	ν (cm^{-1}) MP2[d]	PED[e]	PED B3-PW91	PED B3-LYP	PED B3(M)-LYP	PED
g	662(−3)	664(−4)	676(−5)	661(+3)	δ_{R3}	90	89	82	90
	645	647	642	641					
611(+9)	621(+12)	625(+12)	636(+10)	620(+12)	δ_{R2}	90	89	90	90
	597	609	604	601					
g	427(+13)	428(+11)	436(+7)	289(+9)	τ_{R3}	61	66	73	59
	418	419	419	289	τ_{R2}	20	22	24	20
417(+10)	383(+5)	387(+5)	400(+3)	346(+8)	τ_{R2}	87	86	86	88
	375	379	384	346	τ_{R3}	26	27	28	30

[a] Scaling factor 0.945 for ν(XH), 0.980 for γ and τ, and 0.975 for other vibrational modes. [b] Scaling factor 0.950 for ν(XH), 0.980 for γ and τ, and 0.975 for other vibrational modes. [c] Scaling factor 0.930 for ν(XH), 0.960 for γ and τ, and 0.950 for other vibrational modes. [d] Scaling factor 0.930 for ν(XH), 1.000 for γ and τ, and 0.970 for other vibrational modes. [e] Only contributions >15 are listed; ν^f(OH) and ν^b(OH) indicate the mode of the free OH and of the bonded OH group, respectively. [f] Situated below studied region (<400 cm^{-1}). [g] Intensity too low to be observed.

When the ZPE correction is taken into account, the best agreement between the DFT and MP2 interaction energies is found for the DFT(B3-PW91) method. However, the results computed with DFT(B-LYP) and all other hybrid functionals are also in good agreement with those obtained at the MP2 level of theory.

We also compare in Table 5 the DFT(B3-LYP) interaction energies obtained with different basis sets to determine the basis set dependence of the result. One notices that the BSSE correction is larger for the smaller basis sets which agrees with the results of Novoa et al. [7] and of Hobza et al.[38] The corrections are 0.61, 1.43, and 12.45 kJ/mol with 6-311++G(2d, 2p), 6-31++G**, and 6-31G** basis sets, respectively.

Vibrational Properties. The intramolecular vibrational frequencies calculated for H_2O in the complex are presented in Table 6. The frequency shifts, $\Delta\nu$, for the three H_2O modes with respect to free water are also given.

For the asymmetric (ν_3) and symmetric (ν_1) stretching modes, the comparison between the computed and experimental values is not straightforward, because theses modes have large anharmonicity contributions. As noted in Table 1, the anharmonicity correction for ν_1 is -175 cm^{-1}, which amounts to $\pm 5\%$ of its frequency value. As documented the ν_1 and ν_2 anharmonicities increase in the H-bonded complexes.[39,40]

The symmetric H_2O stretching (ν_1) is directly affected by the H-bond interaction in the complex. The calculated frequency of this mode at the HF level is largely overestimated, while DFT with the S-VWN and S-LYP functionals underestimates its frequency. The frequency calculated with DFT(B-LYP) (3359 cm^{-1}) is very close to the experimental value (3400 cm^{-1}). However, when the anharmonicity correction is taken into account, the calculated frequency decreases and becomes smaller than the experimental value. DFT with all the hybrid functionals yields larger computed frequencies by at least 4% in comparison with the experimental result. The harmonic frequency computed with MP2 is also larger by 6.5% in comparison with the experimental value. The best agreement between the DFT and MP2 is found for the modified B3(M)-LYP functional. The situation is similar for the asymmetric stretching mode. The frequency calculated with DFT(B3(M)-LYP) (3976 cm^{-1}) is very close to the MP2 result (3954 cm^{-1}). One also notices that the frequency ν_1 computed with DFT(B3-LYP)/6-31++G-(2d, 2p) (3542 cm^{-1}) is very close to the value obtained with DFT(B3-LYP)/6-31++G**.

The most important spectral feature, reflecting the formation of the H-bond, is the frequency shift in the H_2O modes. Here we limit the discussion to the frequency shift of the ν_1 mode (see Table 6). The experimental frequency shift for this mode is -271 cm^{-1}. The value obtained using DFT with the B3-LYP/6-31++G** functional (-267 cm^{-1}) is in excellent agreement with the experimental result. The shift, $\Delta\nu_1$, is correctly predicted at all calculation levels, except for the DFT-(S-VWN) and HF levels. It should be mentioned that the frequency shift predicted by DFT(B3(M)-PW91) (-221 cm^{-1}) is also in good agreement with the MP2 predicted value (-230 cm^{-1}).

The frequency shift predicted at the DFT(B3-LYP)/6-31G** level (-169 cm^{-1}) is considerably different from the experimental value, which demonstrates that diffuse orbitals are needed in the basis set to generate reliable vibrational frequency shifts for H-bonded systems. The frequency shift computed at the DFT(B3-LYP) level with 6-311++G(2d, 2p) (-278 cm^{-1}) agrees well with the value calculated using the 6-31++G** basis set. This comparison indicates that additional polarization functions are not needed to reliably reproduce vibrational properties of H-bonded complexes.

The vibrational modes of pyridine groups not directly involved in the H-bond interaction (Tables 7) are only slightly perturbed in the complex. This can be understood because most of these modes involve several pyridine bonds and only small changes occur in the pyridine geometry on H-bond formation. For these modes, the four theoretical methods considered here yield very similar qualitative predictions.

Conclusions

The following conclusions emerge from this study.

The agreement between the calculated and experimental rotational constants for monomeric pyridine increases in the order DFT(B3-PW91) → DFT(B3-LYP) → MP2. This comparison allows to conclude that DFT with the B3-PW91 and B3-LYP functionals are the best methods to study monomeric nucleic acid bases.

The S-VWN and S-LYP DFT functionals are unreliable to study hydrogen-bonded systems. B-LYP/6-31++G** calculations yield reliable interaction energies and intermolecular distances, but they provide an incorrect frequency shift for the ν_1 H_2O mode affected by the H-bond. The hybrid DFT methods yield good results for the intermolecular distances, the interaction energies, and the vibrational frequencies directly influenced by the H-bond interaction in comparison with those obtained with the MP2 method and with the experimental data.

Our analysis demonstrates that the 6-31++G** basis set is sufficient to reliably predict vibrational properties for hydrogen-bonded systems.

The hybrid DFT functionals seem very promising for studying larger, biologically relevant systems where the MP2 method cannot be applied due to a prohibitive computational cost.

Acknowledgment. A. Dkhissi aknowledges the KU Leuven Research Council for a Research Fellowship.

References and Notes

(1) Sim, F.; ST-Amant, A.; Papai, I.; Salahub, D. R. *J. Am. Chem. Soc*. **1992**, *114*, 4391.

(2) Mijoule, C.; Latajka, Z.; Borgis, D. *Chem. Phys. Lett*. **1993**, *208*, 364.

(3) Latajka, Z.; Bouteiller, Y. *J. Chem. Phys*. **1994**, *101*, 9793.

(4) Kim, K.; Jordan, K. D. *J. Phys. Chem*. **1994**, *98*, 10089.

(5) Barone, V.; Adamo, C. *Chem. Phys. Lett*. **1994**, *224*, 43.

(6) Del Bene, J. E.; Person, W. B.; Szczepaniak, K. *J. Phys. Chem*. **1995**, *99*, 10705.

(7) Novoa, J. J.; Sosa, C. *J. Phys. Chem*. **1995**, *99*, 15837.

(8) Xantheas, S. S. *J. Chem. Phys*. **1995**, *102*, 4505.

(9) Lundell, J.; Latajka, Z. *J. Phys. Chem*. **1997**, *101*, 5004.

(10) Rablen, P. R.; Lockman, J. W.; Jorgensen, W. L. *J. Phys. Chem*. **1998**, *102*, 3797.

(11) Destexhe, A.; Smets, J.; Adamowicz, L.; Maes, G. *J. Phys. Chem*. **1994**, *98*, 1506.

(12) Smets, J.; Adamowicz, L.; Maes, G. *J. Mol. Struct*. **1994**, *322*, 113.

(13) Smets, J.; Adamowicz, L.; Maes, G. *J. Phys. Chem*. **1995**, *99*, 6387.

(14) Buyl, F.; Smets, J.; Maes, G.; Adamowicz, L. *J. Phys. Chem*. **1995**, *99*, 14697.

(15) Smets, J.; Adamowicz, L.; Maes, G. *J. Phys. Chem*. **1996**, *100*, 6434.

(16) Smets, J.; Destexhe, A.; Adamowicz, L. Maes, G. *J. Phys. Chem*. **1997**, *101*, 6583.

(17) Van Bael, M. K.; Schoone, K.; Houben, L.; Smets, J.; McCarthy, W.; Adamowicz, L.; Nowak, M. J.; Maes, G. *J. Phys. Chem*. **1997**, *101*, 2397.

(18) Maes, G.; Smets, J.; Adamowicz, L.; McCarthy, W.; Van Bael, M. K.; Houben, L.; Shoone, K. *J. Mol, Struct*. **1997**, *410−411*, 315.

(19) Schoone, K.; Smets, J.; Houben, L.; Van Bael, M. K.; Adamowicz, L.; Maes, G. *J. Phys. Chem*. **1998**, *102*, 4863.

(20) Latajka, Z..; Bouteiller, Y..; Scheiner, S. *Chem. Phys. Lett*. **1995**, *234*, 159.

(21) Dkhissi, A.; Alikhani, M. E.; Bouteiller, Y. *J. Mol. Struct*. **1997**, *416*, 1.

(22) Frisch, C. P. M. J.; Trucks, G. W.; Schlegel, H. B.; Gill, P. M. W.; Johnson, B. G.; Robb, M. A.; Cheeseman, J. R.; Keith, T.; Petersson, G. A.; Montgomery, J. A.; Raghavachari, K.; Al-Laham, M. A.; Zakrzewski, V. G.; Ortiz, J. V.; Foresman, J. B.; Peng C. Y.; Ayala, P. Y.; Chen, W.; Wong, M. W.; Andres, J. L.; Replogle, E. S.; Gomperts, R.; Martin, R. L.; Fox, D. J.; Binkley, J. S.; Defrees, D. J.; Baker, J.; Stewart, J. P.; Head-Gordon, M.; Gonzales, C.; Pople, J. A. *GAUSSIAN 94*, revision B.3; Gaussian Inc.: Pittsburgh, PA, 1995.

(23) Slater, J. C. *Quantum Theory of Molecules and Solids, Vol. 4: The Self- Consistent-Field for Molecules and Solids*; McGraw-Hill: New York, 1974.

(24) Becke, A. D. *Phys. Rev*. **1988**, *A38*, 3098.

(25) Vosko, S. H.; Wilk, L.; Nusair, M. *Can. J. Phys*. **1980**, *58*, 1200.

(26) (a) Lee, C.; Yang, W.; Parr, R. G. *Phys. Rev*. **1988**, *B37*, 785. (b) Perdew, J. P.; Wang, Y. *Phys. Rev*. **1992**, *B45*, 13244.

(27) Johnson, B. G.; Gill, P. M. W.; Pople, J. A. *J. Chem. Phys*. **1993**, *98*, 5612.

(28) Becke, A. D. *J. Chem. Phys*. **1993**, *98*, 1372.

(29) Becke, A. D. *J. Chem. Phys*. **1993**, *98*, 5648.

(30) Becke, A. D. *J. Chem. Phys*. **1988**, *88*, 1053.

(31) Boys, S. F.; Benardi, F. *Mol. Phys*. **1970**, *19*, 553.

(32) Van Duijneveldt, F. B.; Van Duijneveldt-van de Rijdt, J. G. C. M.; van Leuthe, J. H. *Chem. Rev*. **1994**, *94*, 1973.

(33) Rauhut, G.; Pulay, P. *J. Phys. Chem*. **1995**, *99*, 3093.

(34) Person, W. B.; Szczepaniak, K. In *Vibrational Spectra and Structure*; Durig, J. R., Ed.; Elsevier: Amsterdam, 1993; Vol. 2, p 239.

(35) Handy, N. C.; Maslen, P. E.; Amos, R. D.; Andrews, J. S.; Murray, C. W.; Laming, G. J. *Chem. Phys. Lett*. **1992**, *197*, 506.

(36) Goodman, L.; Ozkabak, A. G.; Thakur, S. N. *J. Phys. Chem*. **1991**, *95*, 9044.

(37) Michalska, D.; Bienko, D. C.; Abkowicz-Bienko, A. J.; Latajka, Z. *J. Phys. Chem*. **1996**, *100*, 17786.

(38) Hobza, P.; Sponer, J.; Reschel, T. *J. Comput. Chem*. **1995**, *16*, 1315.

(39) Mijoule, C.; Allavena, M.; Lecloreq, J. M.; Bouteiller, Y. *Chem. Phys*. **1986**, *109*, 207.

(40) Bouteiller, Y.; Latajka, Z.; Ratajczak, H.; Scheiner, S. *J. Chem. Phys*. **1991**, *94*, 2956.

(41) Benedict, W. S.; Gailer, N.; Plyler, E. K. *J. Chem. Phys*. **1956**, *24*, 1139.

(42) Clough, S. A.; Beers, Y.; Klein, G. P.; Rothman, L. S. *J. Chem. Phys*. **1973**, *59*, 2254.

(43) Mills, I. M. In *Theoretical Chemistry*; Dixon, R. N., Ed.; Chemical Society: London, 1974.

(44) Kuchitsu, K.; Morino, Y. *Bull. Chem. Soc. Jpn*. **1965**, *38*, 805.

(45) Sorensen, G. O. *J. Mol. Spectrosc*. **1967**, *22*, 325.

(46) Sorensen, G. O.; Mahler, L.; Rastrup-Andersen, N. *J. Mol. Struct*. **1974**, *20*, 119.